Experimental Investigations of Amino Acid-Layered Double Hydroxide Complexes: Glutamate−Hydrotalcite

Marc X. Reinholdt* and R. James Kirkpatrick

Department of Geology, University of Illinois at Urbana-Champaign, 1301 West Green Street, Urbana, Illinois 61801

Received September 19, 2005. Revised Manuscript Received February 22, 2006

XRD, TGA−DTA, compositional analyses, and ^{13}C NMR data for hydrotalcite (HT) intercalated with the amino acid glutamic acid (GA) provide a detailed picture of the effects of synthesis pH, synthesis temperature, and hydration state on the structure and composition of the GA−HT complexes. GA is most effectively incorporated into HT interlayers at temperatures between 50 and 70 °C and pH values near 10 (pH range 8−12), and much of the GA is adsorbed on HT particle surfaces. $^{1}H-^{13}C$ CP-MAS NMR spectra show that the relative abundance of GA^{-2} anions increases with increasing pH and suggest that at 100% relative humidity (RH), the GA on exterior surfaces occurs in a surface fluid film. The actual GA^{-2}:GA^{-1} ratio, which is close to 1 for a sample synthesized at pH 10, is determined only for a ^{13}C-enriched sample using ^{13}C MAS NMR. At low RH, interlayer GA lies parallel to the layers; at 79% RH, it occurs with its long axis at a high angle to the layers, and at 100% RH, the broad basal reflection at low 2θ values suggests that GA is no longer in simultaneous direct contact with both sides of the interlayer.

Introduction

The interaction of organic and biological species with the surfaces and interlayer galleries of oxide and hydroxide phases is critical in such diverse fields as catalysis, drug delivery, and geochemical transport, but remains incompletely understood.[1−5] Many of these species, including amino acids, carboxylic species, peptides, and larger proteins and natural organic matter (NOM) molecules, occur as anions at neutral to basic pH values and are thus expected to interact strongly with solids having positive structural or pH-dependent charges. Many silicate minerals, such as clays, normally have negative structural charges, but layered double hydroxides (LDHs) do have permanent positive structural charges. The importance of LDH phases in natural and anthropogenic geochemical environments is becoming increasingly clear, and their interactions with organic species are likely to be of considerable significance in these situations.[6−26] LDHs are also receiving increasing attention as potential components of drug delivery systems, in which their interaction with organic and biomolecules is critical.[13−26] Here, we describe an experimental study of the interaction of the amino acids glutamic acid (GA) and glutamine with the prototypical LDH, hydrotalcite (HT; nominally $(Mg_2Al)(OH)_6A^{-}\cdot nH_2O$), that provides significant new insight into the molecular scale interaction of these organic species with LDH phases.[6,9,10,12] X-ray diffraction (XRD), simultaneous thermogravimetric and differential thermal analyses (TGA-DTA), compositional analysis, and ^{13}C and $^{1}H-^{13}C$ magic angle spinning (MAS) and cross-polarization (CP-MAS) nuclear magnetic resonance (NMR) spectroscopy provide data concerning the influence of temperature, pH,

* To whom correspondence should be addressed. E-mail: mreinhol@uiuc.edu. Phone: 217-244-2355. Fax: 217-244-4996.

(1) Bank, S.; Yan, B.; Edwards, J. C.; Ofori-Okai, G. *Langmuir* **1994**, *10*, 1528.
(2) Hill, A. R., Jr.; Böhler, C.; Orgel, L. E. *Origins Life Evol. Biosphere* **1998**, *28*, 235.
(3) Liu, R.; Orgel, L. E. *Origins Life Evol. Biosphere* **1998**, *28*, 245.
(4) Fischer, K. *Water, Air, Soil Pollut.* **2002**, *137*, 267.
(5) Ding, X.; Henrichs, S. M. *Mar. Chem.* **2002**, *77*, 225.
(6) Whilton, N. T.; Vickers, P. J.; Mann, S. *J. Mater. Chem.* **1997**, *7*, 1623.
(7) Fudala, Á.; Pálinkó, I.; Kiricsi, I. *Inorg. Chem.* **1999**, *38*, 4653.
(8) Fudala, Á.; Pálinkó, I.; Hrivnák, B.; Kiricsi, I. *J. Therm. Anal. Calorim.* **1999**, *56*, 317.
(9) Aisawa, S.; Takahashi, S.; Ogasawara, W.; Umetsu, Y.; Narita, E. *J. Solid State Chem.* **2001**, *162*, 52.
(10) Nakayama, H.; Wada, N.; Tsuhako, M. *Int. J. Pharm.* **2004**, *269*, 469.
(11) Yuan, Q.; Wei, M.; Wang, Z.; Wang, G.; Duan, X. *Clay Clay Miner.* **2004**, *52*, 40.
(12) Aisawa, S.; Kudo, H.; Hoshi, T.; Takahashi, S.; Hirahara, H.; Umetsu, Y.; Narita, E. *J. Solid State Chem.* **2004**, *177*, 3987.
(13) Choy, J.-H.; Kwak, S.-Y.; Park, J.-S.; Jeong, Y.-J.; Portier, J. *J. Am. Chem. Soc.* **1999**, *121*, 1399.
(14) Choy, J.-H.; Kwak, S.-Y.; Jeong, Y.-J.; Park, J.-S. *Angew. Chem., Int. Ed.* **2000**, *39*, 4041.
(15) Ambrogi, V.; Fardella, G.; Grandolini, G.; Perioli, L. *Int. J. Pharm.* **2001**, *220*, 23.
(16) Khan, A. I.; Lei, L.; Norquist, A. J.; O'Hare, D. *Chem. Commun.* **2001**, 2342.
(17) Kwak, S.-Y.; Jeong, Y.-J.; Park, J.-S.; Choy, J.-H. *Solid State Ionics* **2002**, *151*, 229.
(18) Ambrogi, V.; Fardella, G.; Grandolini, G.; Nocchetti, M.; Perioli, L. *J. Pharm. Sci.* **2003**, *92*, 1407.
(19) Choy, J.-H.; Jung, J.-S.; Oh, J.-M.; Park, M.; Jeong, J.; Kang, Y.-K.; Han, O.-J. *Biomaterials* **2004**, *25*, 3059.
(20) Tyner, K. M.; Schiffman, S. R.; Giannelis, E. P. *J. Controlled Release* **2004**, *95*, 501.
(21) Tamura, H.; Chiba, J.; Ito, M.; Takeda, T.; Kikkawa, S. *Solid State Ionics* **2004**, *172*, 607.
(22) Wei, M.; Shi, S.; Wang, J.; Li, Y.; Duan, X. *J. Solid State Chem.* **2004**, *177*, 2534.
(23) Li, B.; He, J.; Evans, D. G.; Duan, X. *Appl. Clay Sci.* **2004**, *27*, 199.
(24) del Arco, M.; Cebadera, E.; Gutiérrez, S.; Martín, C.; Montero, M. J.; Rives, V.; Rocha, J.; Sevilla, M. A. *J. Pharm. Sci.* **2004**, *93*, 1649.
(25) Li, B.; He, J.; Evans, D. G.; Duan, X. *Int. J. Pharm.* **2004**, *287*, 89.
(26) Mohanambe, L.; Vasudevan, S. *J. Phys. Chem. B* **2005**, *109*, 15651.

10.1021/cm052107x CCC: $33.50 © 2006 American Chemical Society
Published on Web 04/21/2006

and water content on the structure of the composite materials and provide a basis for future computational studies of the structure, dynamics, and energetics of intercalated and surface glutamate and water molecules.[27−30]

Previous experimental studies of the intercalation of amino acids in LDH compounds have focused principally on the synthesis and characterization of such complexes. In early work, Whilton et al. produced 2:1 Mg:Al hydrotalcite containing aspartic and glutamic acid by coprecipitation at pH 11.5−12 and studied the intercalation of polyaspartate and the thermal polycondensation of aspartic acid.[6] Fudala et al. were the first to use the amphoteric properties of amino acids to intercalate them into previously synthesized NO_3^-−LDH by anion exchange.[7,8] They synthesized tyrosine and phenylalanine Zn−Al LDH at pH 4 and 8 and observed that these phases are thermally less stable than NO_3^-−LDH. Aisawa et al. made a wide range of amino acid LDH phases by direct intercalation during synthesis.[9] Compounds produced included Mg−Al, Mn−Al, Ni−Al, Zn−Al, and Zn−Cr LDHs with phenylalanine and Zn−Al LDH with glycine; alanine; β-alanine; α-, β-, and γ-amino butyric acid; norvaline; valine; norleucine; leucine; isoleucine; phenylglycine; tryptophane; tyrosine; arginine; histidine; aspartic acid; and glutamic acid. More recently, Nakayama et al. used the reconstruction method to produce Mg−Al LDH containing glycine, alanine, valine, leucine, isoleucine, phenylalanine, tryptophan, serine, threonine, cysteine, methionine, proline, asparagine, glutamine, histidine, aspartic acid, glutamic acid, norval, norleucine, aspartame, and several oligoglycines.[10] This method consists of calcination of the precursor LDH at 500 °C, followed by intercalation of the amino acid at ambient temperature and neutral pH. This study also investigated the release of the adsorbed species and demonstrated that LDHs can readily function as amino acid reservoirs and adsorbents. Yuan et al. synthesized Mg−Al LDH with intercalated L-aspartic acid at pH values from 10 to 12 and demonstrated that the optical properties of aspartic acid are unaffected by intercalation.[11] Finally, Aisawa et al. used the reconstruction method with intercalation of the organic species at pH 7.0 and 10.5, producing Zn−Al LDHs containing phenylalanine; leucine; norleucine; norvaline; α-, β-, and γ-amino butylic acid; α- and β-alanine; glycine; arginine; histidine; aspartic acid; and glutamic acid.[12] They also investigated the adsorption rate of phenylalanine.

Materials and Methods

Synthesis. Our samples were synthesized using a coprecipitation method involving hydrolysis of Mg^{2+} and Al^{3+} ions in the presence of glutamic acid or glutamine that is similar to that of Aisawa et al.[9] A mixed solution of 1 M Mg^{2+} and Al^{3+} (2.612 g of $Mg(NO_3)_2{\cdot}6H_2O$ and 1.904 g of $Al(NO_3)_3{\cdot}9H_2O$ completed to 15 g with boiled deionized water) was added dropwise into a 50 mM amino acid solution (0.742 g of glutamic acid completed to 100 g with boiled deionized water) in a boiling flask topped by a condenser. This solution had 2:1:1 Mg^{2+}:Al^{3+}:amino acid molar ratio. The solution pH was adjusted to the required value by the dropwise addition of 1 M NaOH solution, and the mixtures were stirred and refluxed under a nitrogen atmosphere to avoid contamination by atmospheric CO_2. The temperature was controlled by a silicon oil bath. The resulting precipitates were collected by centrifugation after 1 h of reaction, and the solid products were washed with boiled deionized water (DI) and dried under vacuum for 2−3 days. To investigate the influence of synthesis temperature, we synthesized a series of samples at 39, 50, 61, and 72 °C (± 1 °C) and 83 ± 2 °C at an initial pH of 10.0 ± 0.3. The final pH was maintained within 0.3 units of the initial value, except for the 83 °C sample, for which the pH increased to 10.8. To investigate the influence of pH, we synthesized samples at initial pH values of 8.0, 9.0, 10.0, 11.0, and 12.0 (± 0.1) at 50 ± 2 °C. In all cases, the pH decreased 0.2−0.4 units during the synthesis. The water content of LDHs is well-known to affect the interlayer structure and dynamics.[27−30] To study the influence of hydration on glutamate-HT, we synthesized an additional set of samples at pH 9.3, 10.2, and 12.1 at 51 ± 1 °C using the same methods and held them for 6 weeks in closed containers over P_2O_5 (approximately 0% relative humidity, RH), over saturated NH_4Cl solution (RH = 79%), and over DI water (approximately 100% RH); their XRD, TGA-DTA, and $^1H-^{13}C$ CP-MAS NMR data were recorded. To avoid re-equilibration with the ambient atmospheric RH, we quickly introduced the powders into their holders, and the container was sealed if possible (NMR); the experiment was started immediately (TGA-DTA), or paste samples were used when needed (XRD).

Two HT samples containing ^{13}C- and ^{15}N-enriched glutamic acid were synthesized (labeled GA LDH 1 and 2) 12 months apart, at 64 and 65 °C and pH 10.2 and 10.0, respectively, for about 65 min using the same method but at a 2:1:1.2 Mg^{2+}:Al^{3+}:GA molar ratio (instead of 2:1:1). Because of the cost of the enriched GA, the GA used was 1/3 enriched and 2/3 unenriched.

Amino acids and monosodium glutamate monohydrate salt (all L form) were purchased from Acros Organics, $Mg(NO_3)_2{\cdot}6H_2O$ from Sigma, $Al(NO_3)_3{\cdot}9H_2O$ and NaOH from Fisher Scientific, and ^{13}C-enriched glutamic acid from Cambridge Isotopes Lab. All chemicals were used without further analysis.

Analytical Methods. Powder XRD patterns were recorded for all samples from 3 to 10° 2θ or from 3 to 60° 2θ with a step size of 0.02°/point and a rate of 0.5° min^{-1} using a Rigaku rotaflex diffractometer employing Cu Kα radiation (λ = 1.5418 Å), working at 40 kV and 40 mA. Samples were pressed on aluminum holders for analysis, and the relative humidity was 79% unless otherwise noted. Lower-angle XRD data were recorded for some samples on a Philips X'pert diffractometer using Cu Kα radiation, from 0.7 to 25° 2θ with a step size of 0.07°/point and a rate of 1° min^{-1}, working at 45 kV and 40 mA. Samples were pressed on double-faced tape stuck onto a glass slide. Simultaneous thermogravimetric analysis (TGA) and differential thermal analysis (DTA) measurements were carried out using a Netzsch STA 409 thermal analyzer. The samples, typically about 50 mg, were weighed and then rapidly introduced into the cold oven of the instrument. The experiment was started immediately after the balance reached equilibrium. All samples were heated from room temperature to 800 °C at a heating rate of 5 °C min^{-1} under flowing air. For elemental analysis, we determined Al and Mg using an inductively coupled plasma (ICP) emission spectrometer, model OES Optima 2000 DV by Perkin-Elmer. C, H, and N were determined with a CHN analyzer, model CE440 by Exeter Analytical, Inc.

$^1H-^{13}C$ cross-polarization (CP) MAS NMR spectra were obtained at a frequency of 75.435 MHz using a General Electric GN300 wide bore spectrometer (H_0 = 7.05 T) and either a 3.2 or

(27) Hou, X.; Kirkpatrick, R. J. *Chem. Mater.* **2000**, *12*, 1890.
(28) Hou, X.; Kirkpatrick, R. J. *Chem. Mater.* **2002**, *14*, 1195.
(29) Hou, X.; Kalinichev, A. G.; Kirkpatrick, R. J. *Chem. Mater.* **2002**, *14*, 2078.
(30) Hou, X.; Bish, D. L.; Wang, S.-L.; Johnston, C. T.; Kirkpatrick, R. J. *Am. Mineral.* **2003**, *88*, 167.

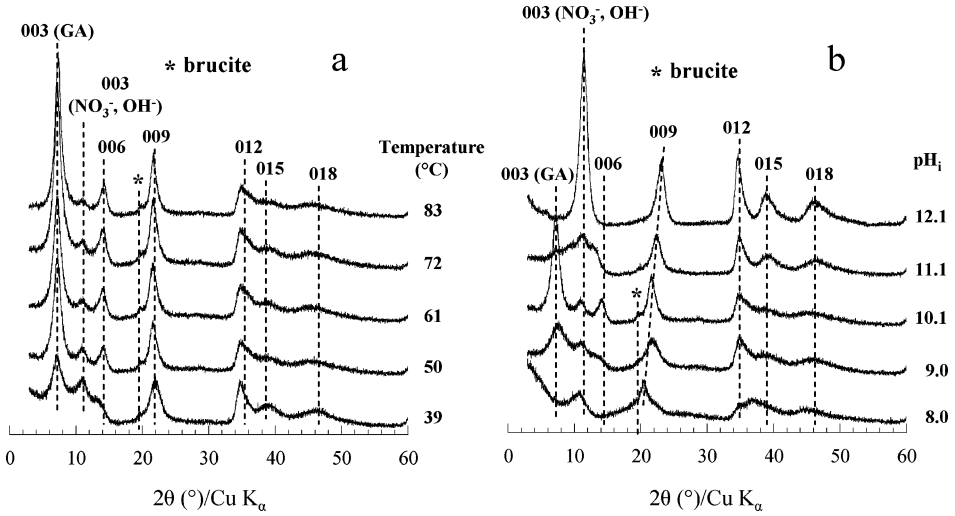

Figure 1. XRD patterns, recorded at 79% RH, of glutamate−hydrotalcite (Mg:Al:GA = 2:1:1) synthesized (a) at pH about 10 and the given temperatures, and (b) at about 50 °C and the given pH values.

7 mm Chemagnetics MAS probe. For samples in the variable-temperature and pH studies, the $^1H-^{13}C$ CP experiments were performed with the 7 mm probe at a MAS frequency of 5 kHz with a contact time of 1000 μs, a relaxation delay of 1.25 s, and a 90° pulse of 6.5 μs. We recorded 5000 transients, and the chemical shifts were referenced to the methyl group of external hexamethyl benzene (HMB) at 17.3 ppm. For the samples in the variable RH study, the $^1H-^{13}C$ CP experiments were performed using the 7 mm probe at a MAS frequency of 5 kHz, a contact time of 2000 μs, a relaxation delay of 2 s, and a 90° pulse of 3.5 μs. We recorded 5000 transients, and the chemical shifts are referenced to the methyl group of external glycine at 43.6 ppm. For the contact time dependence study, the $^1H-^{13}C$ CP experimental conditions of measurement were the same, except they were performed on the ^{13}C-enriched GA LDH 1 sample using the 3.2 mm probe at a MAS frequency of 10 kHz. Single-pulse proton decoupling ^{13}C spectra were acquired for the two ^{13}C-enriched samples at a frequency of 150.760 MHz on a Varian-Oxford Infinity-Plus 600 MHz standard bore spectrometer using a 4 mm Chemagnetics MAS probe. The 90° pulse durations and the relaxation delays for the experiments were 2 μs and 20 s, respectively, the MAS frequency was 6 kHz, 1800 transients were collected, and the chemical shifts were referenced to the methyl group of external tetramethylsilane (TMS) at 0 ppm. Rotors were made of zirconia or silicon nitride and the caps were made of Teflon or Kel-F polymer. After their acquisition, the free induction decay (FID) signals were treated following standard procedures using the NMR Utility Transform Software (NUTS, Acorn NMR software). The background was subtracted (^{13}C MAS only); the baseline was corrected if needed, and the spectra were simulated with the NUTS software.

Results and Interpretation

XRD, TGA−DTA, and Compositions of Synthesized Samples. *Effects of Synthesis Temperature.* XRD shows that the samples synthesized at pH 10 and temperatures from 39 to 83 °C consist of only HT and that for most of the samples, the basal (003) diffraction of the glutamate form (GA−HT) at about 12.2 Å is dominant (Figure 1a). This value is in the range 11.9−12.8 Å previously observed for glutamate Mg−Al and Zn−Al LDHs synthesized under a variety of conditions.[6,9] The peak at about 8.0 Å is the (003) reflection of the NO_3^- form of the LDH and is broadened toward smaller *d*-spacings.[31−34] OH^- may also be intercalated. CO_3^{2-} is a common contaminant of LDHs and is also likely to be present, even though there is no resolved basal peak for it at the expected value of 7.6 Å. The diffraction peaks for the 39 °C sample are broader, indicating a less-ordered sample than at the other temperatures. The intensity of the basal peak for NO_3^-−HT in the 39 °C sample is greater than for the others, indicating less-effective glutamate incorporation than at higher temperatures. The unexpected high intensity of the (009) reflection at about 4.05−4.10 Å relative to the (006) reflection noted for the samples synthesized at pH 10 (Figure 1a) may be due to the superposition of the (009) reflection of GA-LDH and the (006) reflection of NO_3^-−LDH.[24,22]

The TGA−DTA curves of the pH 10 samples are similar and contain features associated with dehydration, dehydroxylation, and combustion of glutamate (Figures 2a, b, and e). There is a weight loss of about 17.0% and there are associated endothermic peaks at temperatures less than 250 °C that are readily assigned to the loss of interlayer and surface water molecules.[31−34] At higher temperatures, there is a larger weight loss of about 36.0% and there are associated endothermic and exothermic features between 300 and 400 °C. Hydrotalcite is well-known to undergo breakdown of the hydroxide layers via dehydroxylation (loss of structural OH^-) in this temperature range.[27−34] For compositions with small inorganic anions such as NO_3^- and CO_3^{2-} in the interlayer, this dehydroxylation is accompanied by a simultaneous loss of anions, creating a poorly ordered mixed-metal oxide, and the associated DTA feature is endothermic.[32,33] For the GA−HT, this dehydroxylation is represented by the endothermic features at about 300 and 390 °C. The large exothermic feature is associated with combustion of the organic molecules and overlaps the central part of the endothermic feature, resulting in the observed pattern.[9,11]

(31) Yun, S. K.; Pinnavaia, T. J. *Chem. Mater.* **1995**, *7*, 348.
(32) Constantino, V. R. L.; Pinnavaia, T. J. *Inorg. Chem.* **1995**, *34*, 883.
(33) Aramendía, M. A.; Avilés, Y.; Benítez, J. A.; Borau, V.; Jiménez, C.; Marinas, J. M.; Ruiz, J. R.; Urbano, F. J. *Microporous Mesoporous Mater.* **1999**, *29*, 319.
(34) Zhao, Y.; Li, F.; Zhang, R.; Evans, D. G.; Duan, X. *Chem. Mater.* **2002**, *14*, 4286.

Table 1. Analyzed Chemical Compositions and Atomic Molar Ratios of Glutamate−Hydrotalcite Samples Synthesized at the Listed pHs and 50 °C

	amount (wt %)					atomic molar ratios			
pH	C	H	N	Mg	Al	Mg/Al	N/Al	C/Al	C/N
8.0	4.43	3.77	3.14	14.82	8.84	1.86	0.68	1.13	1.66
9.0	5.53	3.78	2.98	15.16	8.42	2.00	0.68	1.47	2.16
10.1	5.84	3.62	2.85	15.11	7.78	2.15	0.70	1.69	2.41
11.1	4.39	3.64	2.14	17.43	8.53	2.27	0.48	1.16	2.42
12.1	2.29	3.74	1.38	19.35	8.91	2.41	0.30	0.58	1.93

Complete combustion of GA occurs at temperatures below 500 °C in the LDH, whereas combustion of crystalline glutamic acid is complete only at 580 °C (our data, not shown). On the other hand, the total combustion of the δ-COO^- and of the C_0-COO^- monosodium glutamate salts occurs at about 450 [35] and 480 °C (our data, not shown), respectively. Thus, GA intercalated in HT is less thermally stable than glutamic acid but slightly more so than the monosodium glutamate salts.

Effect of Synthesis pH. The pH of synthesis has a much more significant effect on the GA−HT structure than does temperature at pH ca. 10. The XRD patterns of the samples synthesized at pH 8.0−12.1 contain the characteristic 00*l* and 0*kl* diffractions of LDHs, but the positions and intensities of the basal spacings vary greatly (Figure 1b). The 12.2 Å basal diffraction of GA−HT is detectable only at pH values of 9.0, 10.1, and 11.1, and this peak is dominant only at pH 10.1. All the samples also yield (003) peaks between 7.7 and 8.2 Å for NO_3^-− or OH^-−LDH, although the pH 8.0 sample is poorly crystallized. At pH 8.0, 9.0, and 10.1, observed basal spacings of 8.0−8.2 Å suggest that the dominant interlayer species is NO_3^-, whereas at pH 12.1, the basal spacing of 7.7−7.9 Å suggests that OH^- dominates, as expected at this high pH. In contrast, Whilton et al.[6] observed significant GA incorporation in Mg−Al LDH at high pH values (11.5−12), with a basal diffraction of 11.9 Å, although their synthesis involved adding the metal nitrate solution to the glutamate solution, which is the opposite of our sequence (see the Experimental Section). Aisawa et al. observed basal reflections of 12.7 and 12.8 Å for GA intercalated in Zn−Al LDH synthesized by the coprecipitation[9] method at pH 8 and the reconstruction[12] method, respectively.

The analyzed compositions of our samples show an increase in the Mg:Al ratio with increasing pH (Table 1). A Mg:Al ratio of 1.86 for the pH 8.0 sample is consistent with the observed poor crystallinity, because the minimum Mg:Al ratio for HT without Al−O−Al bonds is 2.0, which is generally considered the limiting ratio for LDHs.[31,36,37] The N:Al ratios are nearly constant at pH 8.0−10.1 and are significantly lower at pH 11.1 and 12.1. There is a significant C content at all pH values, with a maximum of the C:Al ratio at 10.1. As for the N:Al ratio, the C:Al ratio decreases significantly at the highest pH values. The occurrence of the maximum C content at pH 10.1 is consistent with the strong (003) diffractions for GA−HT at this pH. The pH 8.0 and 9.0 samples are poorly crystallized; part of their Mg and Al may occur in phases other than LDH, and the pH 12.1 sample contains substantial CO_3^{2-} and OH^-. The C:N ratios of 1.66−2.42 are quite low compared to the glutamate C:N ratio of 5, which shows that all samples contain significant amounts of NO_3^- and is consistent with the presence of corresponding (003) diffractions on XRD patterns. Nonetheless, the high C content suggests the presence of glutamate in all these samples. The absence of basal diffractions for GA−HT for some of them suggests that much of the glutamate is on particle surfaces. Structurally, glutamic acid consists of an amino headgroup, a 2C alkyl chain, and two terminal carboxylic groups, as shown in Scheme 1. The pK_a values of the carboxylic groups are low (2.16 for the backbone amino acid (C_0) and 4.15 for δ-COOH/δ-COO^-), and thus the groups are deprotonated (COO^-) at the pH values of our syntheses. For the amine group, however, pK_b = 9.58 (NH_3^+/NH_2); in solution, the −1 anion ($C_5H_7NO_4^-$) should be dominant at a pH less than this value and the −2 anion ($C_5H_6NO_4^{2-}$) at higher pH values. Because of the coexistence of several LDH phases in the same sample, it is not possible to determine their chemical formulas.

Scheme 1. Structure of Glutamic Acid[a]

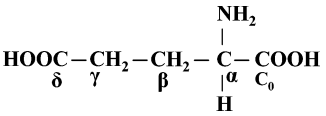

[a] pK_a = 2.16 ($COOH/COO^-$), pK_b = 9.58 (NH_3^+/-NH_2), pK_c = 4.15 (δ-COOH/δ-COO^-), pI = 3.22 (isoelectric point)

The TGA−DTA patterns for these samples also vary with pH (Figure 2); but, importantly, all show the presence of significant amounts of glutamate, even though XRD does not show separate basal diffractions for a phase with it in the interlayer. The TGA−DTA curves for the pH 9.0, 10.1, and 11.1 samples are very similar to the 39 and 72 °C pH 10 samples described above, and the assignment of the features is the same: low-temperature dehydration followed at higher temperature by dehydroxylation, combustion of organics, and loss of small interlayer species (NO_3^-, OH^-, and any CO_3^{2-}). For the pH 8.0 sample, dehydroxylation and combustion occur over a broader range of temperatures starting near 220 °C and continuing to 400 °C, consistent with its more disordered structure. The improved resolution of the high-temperature endothermic features for the pH 11.1 sample and especially for the pH 12.1 sample is probably due to a decrease in the proportion of glutamate relative to other counteranions, in agreement with XRD and compositional results. The pH 12.1 sample also shows reasonably well-resolved endothermic features near 170 and 240 °C that are probably due to the loss of water molecules in pores (interparticle water due to capillary condensation), on the surface, and/or in the interlayer, as shown by Yun and Pinnavaia for CO_3^{2-}−LDH[31] and LDH with various anions by Constantino and Pinnavaia[32] and Zhao et al.[34]

The LDH samples synthesized using the amino acid glutamine at the same pH values and using the same methods as for the GA−HTs described above yield no basal X-ray

(35) Vlase, T.; Vlase, G.; Doca, N. *J. Therm. Anal. Calorim.* **2005**, *80*, 425.
(36) Weir, M. R.; Kydd, R. A. *Microporous Mesoporous Mater.* **1998**, *20*, 339.
(37) Villegas, J. C.; Giraldo, O. H.; Laubernds, K.; Suib, S. L. *Inorg. Chem.* **2003**, *42*, 5621.

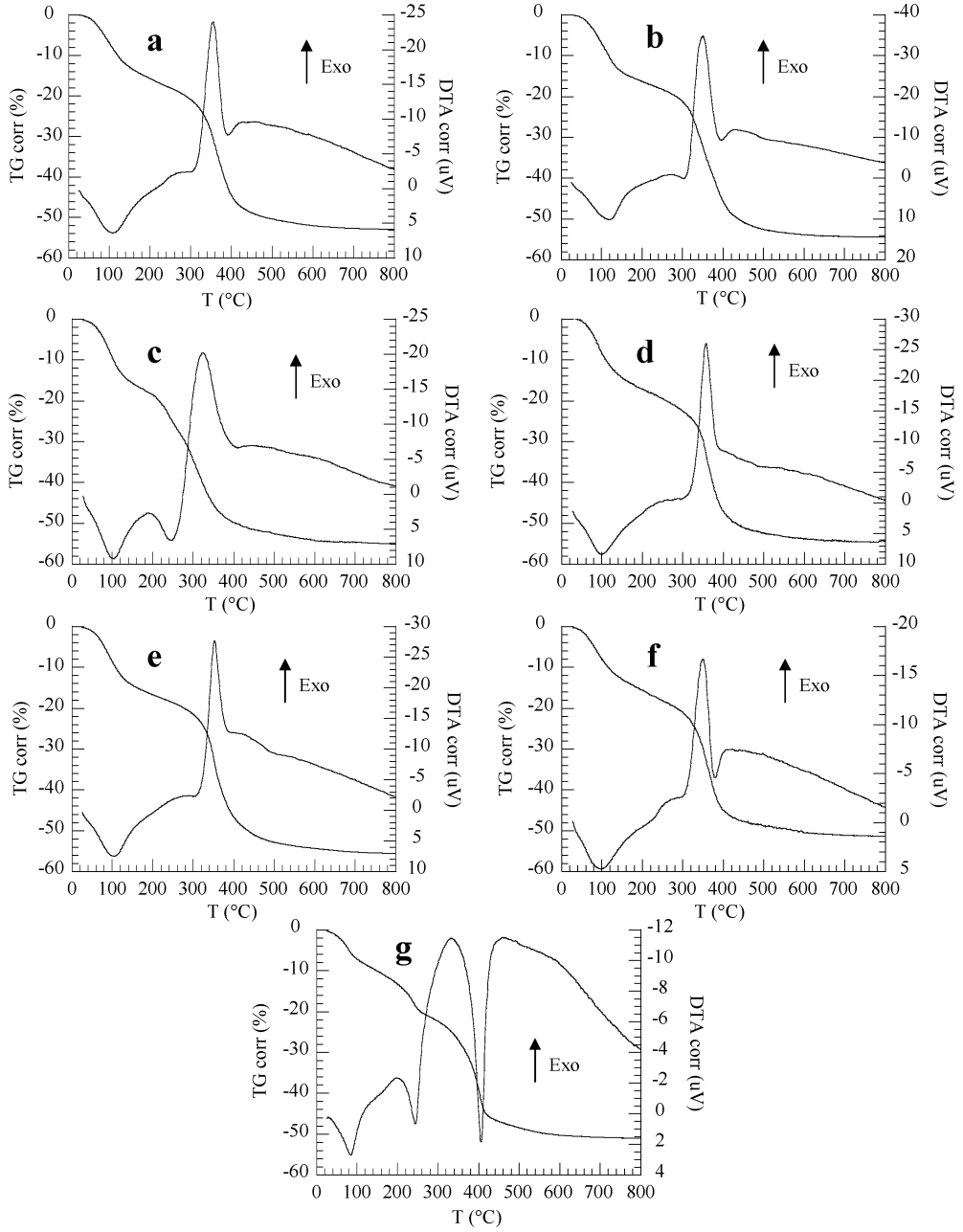

Figure 2. Representative TGA−DTA patterns of glutamate−hydrotalcite synthesized at pH 10 and (a) 39 or (b) 72 °C, or at about 50 °C and pH values of (c) 8.0, (d) 9.0, (e) 10.1, (f) 11.1, and (g) 12.1.

diffractions larger than those corresponding to NO_3^-−, OH^-− or CO_3^{2-}−HT. Nor do they show exothermic features for glutamine combustion in the DTA patterns or ^{13}C NMR spectra (data not shown). We conclude that glutamine is not intercalated in or sorbed on the surfaces of HT under our synthesis conditions. Glutamine differs from glutamic acid by the substitution of an amide group for the δ carboxylic group (CO−NH_2 instead of COOH, refer to Scheme 1). Thus, the lateral chain of the molecule does not possess any acidic or basic properties, and the only possible sites of negative and positive charge development in the molecule are the carboxylic group and the amine group of the amino acid motif. The differences in HT sorption of glutamate and glutamine by HT suggest that the sorption interactions are dominated by the functional groups of the alkyl chain and that the functional groups of the amino acid motif are less significant.

Table 2. Basal (003) *d*-spacings (Å) at the Listed Relative Humidity (RH) for Glutamate−Hydrotalcite Samples Synthesized at the Listed pHs and 50 °C[a]

	d-spacing (Å)		
pH	100% RH	79% RH	dry
9.3	7.8 (15−29^{vw}, 7.7^{s})	11.7, 7.8	8.2
10.2	7.7 (16−28^{vw}, 7.6^{s})	11.5, 7.8	11.5^{s}, 8.5
12.1	7.3	7.6	7.6

[a] Values in parentheses are those observed for data recorded at lower 2θ angles. Letters stand for the following: s, small; vw, very weak.

Effect of Relative Humidity. The XRD data for samples synthesized at 51 °C and pH 9.3, 10.2, and 12.1 show that the basal spacing of GA−HT depends greatly on RH and that the maximum expansion is greater than that observed for LDHs with small inorganic anions;[27−30] they also confirm the absence of interlayer glutamate at pH 12.1 (Table 2). The pH 9.3 sample yields a single basal (003) diffraction at

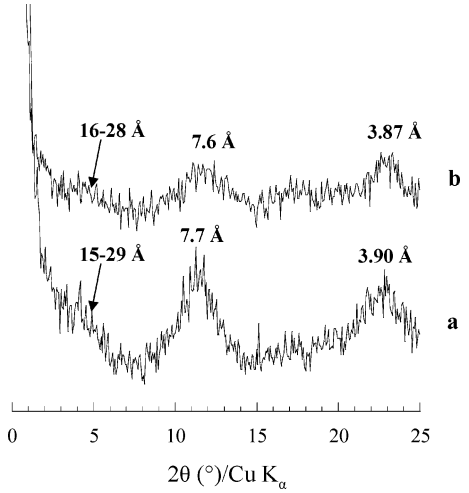

Figure 3. Low-angle XRD patterns of glutamate−hydrotalcite (Mg:Al: GA = 2:1:1) synthesized at pH (a) 9.3 and (b) 10.2.

8.2 Å under dry conditions. At 79% RH, this splits into peaks at 11.7 (GA−HT) and 7.8 Å (NO_3^-−HT); at 100% RH, only a peak for NO_3^- − HT at 7.5 Å and perhaps the tail of a peak at low 2θ are visible (see low-angle XRD data below). The patterns of the pH 10.2 sample are generally similar, except that the dry sample yields a small peak near 11.5 Å for GA−HT. Low-angle XRD data for the pH 9.3 and 10.2 samples equilibrated at 100% RH show very broad weak peaks in the 15−30 Å range for the (003) GA−HT band for both samples (Figure 3). The (003) NO_3^-−HT peak at about 7.7 Å is much stronger relative to the intensity of the (003) GA−HT peak than for the same sample equilibrated at 79% RH. The increasing basal spacing of the GA−HT from ca. 8.5 to 11.5 Å from dry to 79% RH conditions suggests possible reorientation of the glutamate molecule from being parallel to the hydroxide layers to being at a high angle to them. The glutamate ion is approximately 4.6 Å thick by 7.5 Å long, and this change in orientation is consistent with the 3 Å increase in basal spacing. Similar reorientation occurs for tartrate and terephthalate intercalated into LDHs.[38,39] Basal spacings of 15−30 Å at 100% RH clearly indicate significant expansion due to water intercalation and suggest that, under these conditions, the GA molecules cannot be simultaneously in contact with both sides of the interlayer. The increased peak widths indicate increased basal spacing disorder.

The TGA−DTA data for the pH 9.3, 10.2, and 12.1 samples equilibrated at different RH clearly demonstrate increasing water content at increasing RH, the similarity of the pH 9.3 and 10.2 samples, and the presence of glutamate even in the pH 12.1 sample (Figure 2, Table 3). For the pH 9.3 and 10.2 samples, the curves are very similar to those for the other samples synthesized near pH 10 described above, except that the magnitudes of the weight losses and endothermic features at temperatures less than 200 °C due to loss of molecular water increases greatly with increasing RH, paralleling the increase in XRD basal spacing for GA−HT. The apparent magnitudes of the high-temperature weight losses increase with decreasing RH because of the decreasing concentration of water molecules. The TGA−DTA curves of the pH 12.1 sample are quite different, reflecting the lower concentration of GA and the dominance of OH^- in the interlayer. Again, the low-temperature weight loss centered near 90 °C decreases with decreasing RH, reflecting lower water contents. These samples also yield a well-resolved weight loss of 9−13% and an endothermic peak at 240 °C due to interlayer and surface water, as was previously observed for LDHs with several different counteranions, including CO_3^{2-}, OH^-, SO_4^{2-}, and Cl^-.[31,32,34]

Table 3. Thermogravimetric Analysis Data Obtained at the Listed Relative Humidities (RH) for Glutamate−Hydrotalcite Samples Synthesized at the Listed pH Values and 50 °C

RH (%)	*T* range (°C)	weight loss (%)
	pH 9.3	
100	25−250	35
100	250−800	31
79	25−250	16
79	250−800	40
dry	25−800	48
	pH 10.2	
100	25−250	38
100	250−800	30
79	25−250	18
79	250−800	39
dry	25−800	48
	pH 12.1	
100	25−150	31
100	150−300	9
100	300−800	20
79	25−150	8
79	150−300	13
79	300−800	29
dry	25−300	12
dry	300−800	32

^{13}C NMR Results. The ^{13}C NMR results show the presence of glutamate in all the GA−HT samples and are consistent with the expected increase in the GA^{-2}:GA^{-1} ratio with increasing pH and the interpretations of the compositional, XRD, and TGA−DTA data described above. The ^{1}H−^{13}C CP-MAS spectra of the as-received crystalline glutamic acid and monosodium glutamate monohydrate (not shown) provide a basis for interpreting the spectra of the GA−HT samples. The spectrum of glutamic acid contains peaks at 180.4 and 178.5 ppm that correspond to the δ-COOH and C_0−COOH of the amino acid unit, respectively, a peak at 55.1 ppm that corresponds to the α-carbon bearing the amino group (α-$CHNH_2$), and two peaks at 25.8 and 23.9 ppm that correspond to signals for the β- and γ-carbons of the alkyl chain, respectively (β- and γ-CH_2).[40−42] The spectrum of monosodium glutamate monohydrate is more complex and contains three carboxylate resonances at 181.1, 179.7, and 175.1 ppm; two peaks in the α-$CHNH_2$ region at 54.1 and 52.9 ppm; and three peaks in the CH_2 region at 38.3, 34.0, and 26.5 ppm. To the best of our knowledge, the structure of this compound is not known, and detailed assignment of these resonances is beyond the scope of this paper. It is likely,

(38) Prevot, V.; Forano, C.; Besse, J. P.; Abraham, F. *Inorg. Chem.* **1998**, *37*, 4293.
(39) Newman, S. P.; Williams, S. J.; Coveney, P. V.; Jones, W. *J. Phys. Chem. B* **1998**, *102*, 6710.
(40) Horsley, W.; Sternlicht, H.; Cohen, J. S. *J. Am. Chem. Soc.* **1970**, *92*, 680.
(41) Quirt, A. R.; Lyerla, J. R., Jr.; Peat, I. R.; Cohen, J. S.; Reynolds, W. F.; Freedman, M. H. *J. Am. Chem. Soc.* **1974**, *96*, 570.
(42) Evans, C. A.; Rabenstein, D. L. *J. Am. Chem. Soc.* **1974**, *96*, 7312.

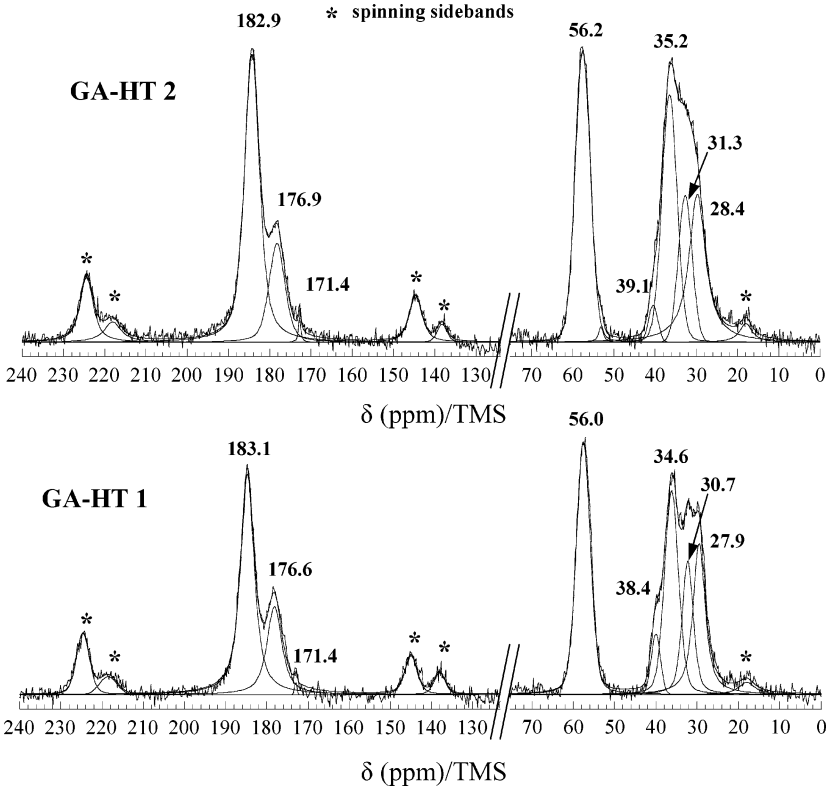

Figure 4. ^{13}C MAS NMR spectra of glutamate−hydrotalcite samples synthesized with 33% ^{13}C-enriched glutamic acid at pH 10.2 and 64 °C (GA−HT 1) and at pH 10.0 and 65 °C (GA−HT 2).

however, that the differences with glutamic acid are due to the Na and H_2O.

HT made with ^{13}C-Enriched Glutamic Acid. The ^{13}C MAS NMR spectra of the ^{13}C-enriched samples made at pH 10.2 and 64 °C (GA−HT 1) and at pH 10.0 and 65 °C (GA−HT 2) contain resonances for the β-CH_2, γ-CH_2, α-$CHNH_3^+$/NH_2, C_0-COO^-, and δ-COO^- groups of glutamate along with CO_3^{2-}, and the relatively high signal:noise ratio of the spectra allows for effective assignment of the resonances of GA^{-1} and GA^{-2} (Figure 4). These assignments are in agreement with the more-extensive $^1H-^{13}C$ CP-MAS data for our samples described below. The room humidity XRD patterns of these samples are essentially identical to those of the other samples made near pH 10, showing a large basal peak for GA−HT near 12.2 Å (data not shown). The basal peaks for NO_3^-− and OH^-−HT near 8.0 Å are somewhat larger for these samples than for the samples with unenriched glutamate. Experiments investigating the effects of excess glutamic acid show that this does not perceptibly change the final material (data not shown).

The ^{13}C NMR spectra of these samples contain peaks for COO^- at about 183.0 and 176.7 ppm that are about 4.5 ppm broad at half-height and contain a total of about 40% of the total signal (Table 4). In the α-$CHNH_2/NH_3^+$ region near 56 ppm, there is a single resonance that is 4.5 ppm broad and contains 18−20% of the total signal. In the ethyl region (β- and γ-CH_2), there are broad peaks or shoulders at about 28, 31, and 35 ppm that contain about 38% of the total intensity. Within the error of fitting such broad peaks, the peak areas are consistent with the expected 2:1:2 ratio for $C_0-COO^- + \delta$-COO^-: α-$CHNH_2/NH_3^+$: β-$CH_2 + \gamma$-CH_2 of glutamate. Most of these peaks are readily assigned (Table 4) on the basis of the peak areas and the known pH dependence of the ^{13}C NMR resonance of amino acid ions in solution. Quirt et al.[41] have shown that the chemical shifts of all the C sites of glutamate in aqueous solution become less shielded (more positive) with increasing pH across the pK_a of the amine group near pH 9.5, but that the amount of change is different for each of the sites. For the C_0-COO^- carbon, $\delta^{13}C$ changes from 175 ppm at pH 8 (mostly GA^{-1}) to nearly 184 ppm at pH 12 (mostly GA^{-2}). For the δ-COO^- carbon, the comparable change is smaller, from 181.9 to 183.5 ppm (Figure 5c). For the α-$CHNH_3^+/NH_2$ carbon, it is only from 55.5 to 56.8 ppm (Figure 5a); for the β-CH_2,

Table 4. ^{13}C MAS NMR Data for ^{13}C-Enriched Glutamate−Hydrotalcite Synthesized at pH 10.2 and 64 °C (GA-HT 1) and pH 10.0 and 65 °C (GA-HT 2)

component	chemical shift[a] (ppm)	fwhm (Hz)	relative peak area (%)
	GA-HT 1		
β-CH_2 (GA^{-1})	27.9	520	12.4
β-CH_2 (GA^{-2})	30.7	480	8.8
γ-CH_2	34.6	600	15.0
Na−CH_2 [b]	38.4	400	2.8
α-$CHNH_2/NH_3^+$	56.0	605	17.8
CO_3^{2-}	171.4	100	0.1
C_0-COO^- (GA^{-1})	176.6	650	12.0
δ-COO^- and C_0-COO^- (GA^{-2})	183.1	600	28.4
	GA-HT 2		
β-CH_2 (GA^{-1})	28.4	720	14.3
β-CH_2 (GA^{-2})	31.3	600	8.1
γ-CH_2	35.2	650	15.5
Na−CH_2[b]	39.1	400	1.4
α-$CHNH_2/NH_3^+$	56.2	650	19.6
C_0-COO^- (GA^{-1})	176.9	685	10.3
δ-COO^- and C_0-COO^- (GA^{-2})	182.9	650	30.0

[a] The chemical shift assignments are based on those of ref 41. [b] The chemical shift may be due to the presence of sodium glutamate species.

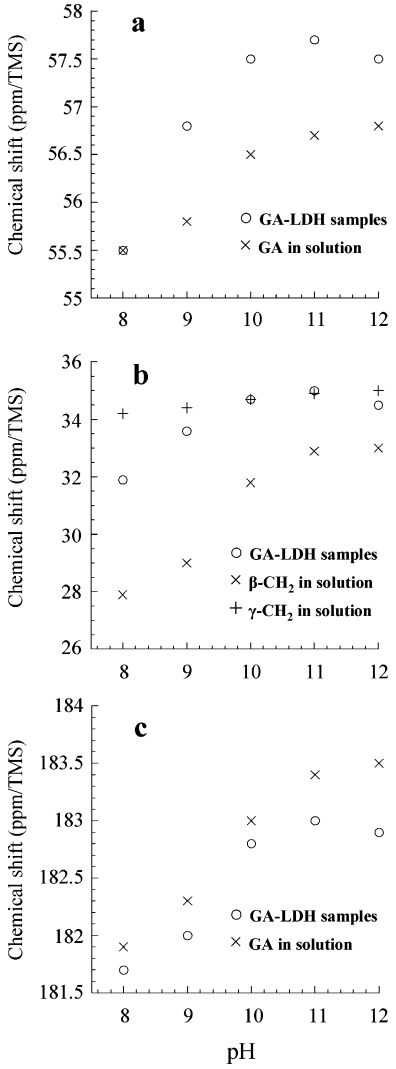

Figure 5. ^{13}C chemical shifts of (a) α-$CHNH_3^+/NH_2$, (b) β- and γ-CH_2, and (c) δ-COO^- sites in glutamate−hydrotalcite plotted vs pH of synthesis and compared to values for 0.1 g mL^{-1} aqueous solutions of glutamic acid.

from 28.0 to 33.0 ppm; and for the γ-CH_2, from 34.2 to 35 ppm (Figure 5b). The only peak in the spectra of the isotopically enriched GA−HT samples that cannot be assigned is the one near 38.5 ppm, which accounts for 1.4 and 2.8% of the total signal intensity. Its position suggests that it is due to a CH_2 site, but the value is too positive for it to be due to any such site in glutamic acid at any pH. The presence of a resonance near 38 ppm for monosodium glutamate monohydrate allows us to speculate that it may be due to a Na−glutamate site. The presence of a small peak near 171.4 ppm for CO_3^{2-} in both samples suggests a quite large amount of CO_3^{2-}, because it is not isotopically enriched. The relative areas of the peaks for GA^{-1} and GA^{-2} in the carboxylate region (more-precise simulation than for the CH_2 region) show that the GA^{-2}:GA^{-1} ratios are 0.9 and 1.0 for GA−HT 1 and 2, respectively. At the pH of synthesis (about 10), the GA^{-2}:GA^{-1} ratio in solution is expected to be greater than 1, and because LDHs containing inorganic anions often show a preference for the higher-charge species, this result seems anomalous.[27−30,43] Leucine intercalation in Mg−Al LDH, however, shows comparable preferential incorporation of the lower-charged species and was also accompanied by a significant amount of CO_3^{2-} in the sample.[10]

Table 5. Cross-Polarization Parameters for the Listed Sites of Glutamate−Hydrotalcite Synthesized with ^{13}C-Enriched Glutamic Acid (GA LDH 1 sample), Obtained from the Fitted Intensities of the $^1H-^{13}C$ CP-MAS Spectra of These Samples

signal	T_{CH} (ms)	$T_{1\rho}^H$ (ms)	$I_0 \times 10^{-6}$ (a.u.)
α-$CHNH_3^+$	0.07 ± 0.01	2.7 ± 0.2	236 ± 8
α-$CHNH_2$	0.10 ± 0.01	1.3 ± 0.1	151 ± 5
β-CH_2	0.07 ± 0.01	1.7 ± 0.1	270 ± 8
γ-CH_2	0.05 ± 0.01	1.7 ± 0.1	558 ± 16
δ-COO^-	0.65 ± 0.03	8.2 ± 1.1	330 ± 11
C_0-COO^- [a]	0.69 ± 0.21	9.1 ± 8.5	125 ± 25

[a] This signal had a poor-quality regression.

The contact time dependences of the resonances for the isotopically enriched sample GA LDH 1 at room humidity obtained for the $^1H-^{-3}C$ CP-MAS spectra demonstrate that the α-$CHNH_2$, β-CH_2, and γ-CH_2 sites cross-polarize much more efficiently than the COO^- sites (spectra not shown). This behavior is due principally to the presence of C−H bonds for the α-$CHNH_2$, β-CH_2, and γ-CH_2 sites, because the CP efficiency is related to the dipolar coupling between these nuclei, which varies as $1/r_{jk}^3$.[44,45] Fitting of the contact time (t) dependences using the standard relationship $I(t) = I_0(1 - T_{CP}/T_1\rho^H)^{-1}[\exp(-t/T_1\rho^H) - \exp(-t/T_{CP})]$,[46−48] where I_0 is the peak intensity, T_{CH} is the cross-polarization time between protons and carbons, and $T_1\rho^H$ is the proton spin−lattice relaxation time in the rotating frame, gives the values listed in Table 5. As expected, the $T_1\rho^H$ values of the carboxylate carbons are longer than for the other carbons, because they do not bear any proton. The T_{CP} values of the carboxylate carbons are also much longer than those of the other carbons, because T_{CP} decreases with both decreasing proton−carbon distance and increasing number of protons interacting with the carbon under observation[46,48] and increases with increasing mobility of a structural fragment bearing this carbon.[46] Although α-CHN carbons bear only one proton and we might expect a significantly longer T_{CP} than for the CH_2 carbons, the values for the α-CHN carbons are all short, in the range of 0.05 ms. These short values are probably due to the effects of the hydrogen borne by the nitrogen atom. The slightly longer T_{CP} value for α-$CHNH_2$- than for α-$CHNH_3^+$ supports this assessment. These observations show that interaction of the glutamate with the LDH hydroxide layers do not significantly affect the local bonding environments of the carbons.

$^1H-^{13}C$ CP-MAS NMR of Unenriched GA−HT Samples. The GA−HT samples made with isotopically unenriched glutamic acid do not yield ^{13}C MAS NMR spectra with useful signal:noise ratios, but the $^1H-^{13}C$ CPMAS spectra provide

(43) Hou, X.; Kirkpatrick, R. J.; Yu, P.; Moore, D.; Kim, Y. *Am. Mineral.* **2000**, *85*, 173.
(44) Harris, R. K. *Nuclear Magnetic Resonance Spectroscopy*; Longman Scientific & Technical: Harlow, U.K., 1986.
(45) Levitt, M. H. *Spin Dynamics Basics of Nuclear Magnetic Resonance*; J. Wiley & Sons: Chichester, England, 2001.
(46) Wawer, I.; Nartowska, J.; Cichowlas, A. A. *Solid State Nucl. Magn. Reson.* **2001**, *20*, 35.
(47) Conte, P.; Piccolo, A.; van Lagen, B.; Buurman, P.; Hemminga, M. A. *Solid State Nucl. Magn. Reson.* **2002**, *21*, 158.
(48) Pisklak, M.; Kossakowski, J.; Perliński, M.; Wawer, I. *J. Mol. Struct.* **2004**, *698*, 93.

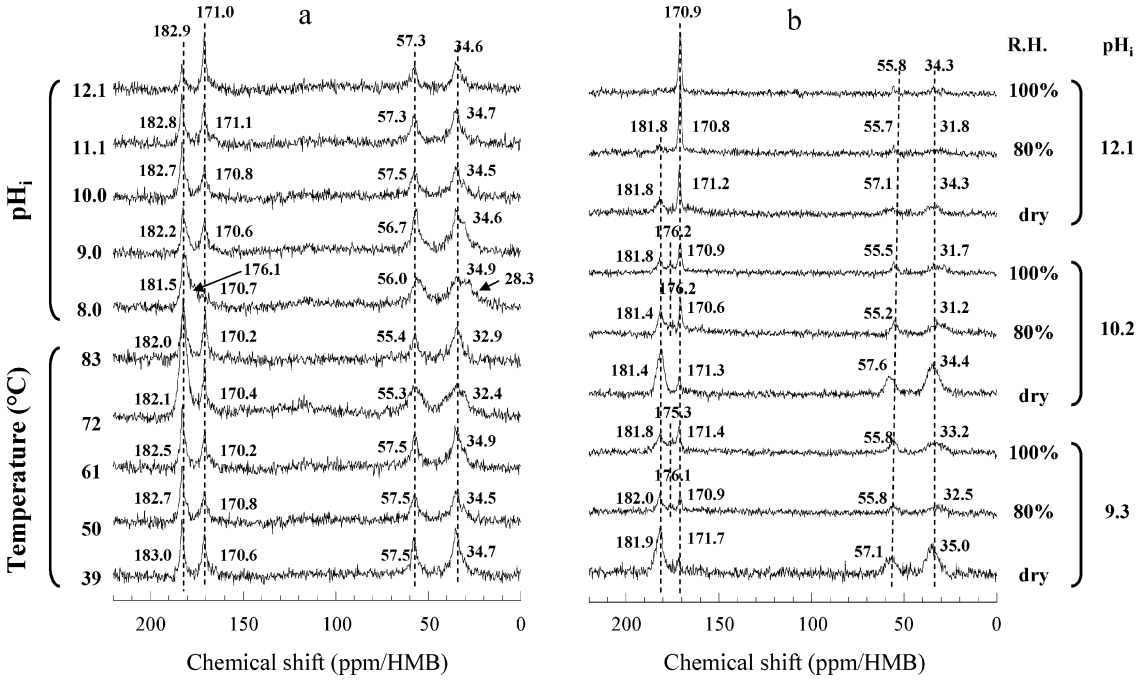

Figure 6. $^{1}H-^{13}C$ CP-MAS spectra of glutamate−hydrotalcite (a) synthesized at various pHs and about 50 °C, or at various temperatures and pH about 10.0, or (b) synthesized at various pHs and about 50 °C and recorded after equilibration at the indicated relative humidity.

insight into the effects of pH, synthesis temperature, water content, and thermal history on GA−HT (Figure 6). In all cases, the only signals detected are for glutamate and CO_3^{2-}.

Effect of Synthesis pH. For the samples synthesized at 50 °C and pH from 8.0 to 12.1, the relative intensities of the resonances for GA^{-2} and CO_3^{2-} increase with increasing pH. In all cases, there is signal near 34.5 ppm for γ-CH_2 in GA^{-1} or GA^{-2}, near 56−57 ppm for α-$CHNH_3^+/NH_2$ in GA^{-1} or GA^{-2}, near 182 pm for δ-COO^- in GA^{-1} or GA^{-2} and C_0-COO^- in GA^{-2}, and near 171 ppm for CO_3^{2-}. For the pH 8.0 sample, there is also a signal for β-CH_2 and C_0-COO^- in GA^{-1} at 28.3 and 176.1 ppm, respectively. For the pH 9.0 sample, there is a shoulder near 28.3 ppm for β-CH_2 in GA^{-1}. The peak maxima in the COO^- (181.5−182.9 ppm) and α-$CHNH_2/NH_3^+$ (56.0−57.5 ppm) regions and the centers of gravity of the β- and γ-CH_2 regions become significantly more positive with increasing pH. These variations parallel the trends for glutamic acid in solution,[41] for which the signals represent the average chemical shifts of the GA^{-1} and GA^{-2} due to rapid proton exchange (Figure 5). GA^{-2} is, thus, present at all pH values, and at pH 10.0, 11.1, and 12.1, the only well-resolved signals are for GA^{-2} and CO_3^{2-}.

Effect of Synthesis Temperature. For the GA−HT samples synthesized at pH 10 and temperatures from 39 to 83 °C, the $^{1}H-^{13}C$ CPMAS spectra are nearly identical, showing signals for only GA and CO_3^{2-} (Figure 6). GA^{-2} appears to be the dominant GA species.

Effect of Relative Humidity (water content). Increasing RH for the 50 °C, pH 9.3, 10.2, and 12.1 samples results in decreasing relative $^{1}H-^{13}C$ CP-MAS intensity for the signals from the glutamate and increasing relative intensity for CO_3^{2-} (Figure 6). In general, the GA peaks for the dried samples are broad and poorly resolved, and for the pH 9.3 and 10.1 samples, resolution of the COO^- signals for the GA^{-1} and GA^{-2} resonances is slightly better at higher RH values. The total signal for GA in the pH 12.1 sample is quite weak, reflecting its low GA content.

The decreasing $^{1}H-^{13}C$ CP-MAS signal intensity for GA at 79 and 100% RH demonstrates increased dynamic decoupling of the ^{1}H and ^{13}C spin systems at high water contents. The nearly total loss of signal for the pH 12.1 sample, which has essentially no interlayer glutamate, at 100% RH suggests that the GA on the exterior surfaces of HT particles enters the surface fluid film that forms under these conditions and is fully self-decoupled, as in bulk aqueous solution. The decrease in $^{1}H-^{13}C$ CP-MAS signal intensity for GA at 100% RH for all the samples suggests that much of their GA occurs on exterior particle surfaces. The XRD data for samples at pH values near 9 and 10 show increased basal spacings at 100% RH because of the intercalation of water, but the presence of a $^{1}H-^{13}C$ CP-MAS signal intensity for them indicates that interlayer GA does not undergo sufficient reorientational motion to eliminate the $^{1}H-^{13}C$ dipolar couplings.

Conclusions

Together, the XRD, TGA−DTA, compositional, and NMR data for our samples provide a quite detailed picture of the structure of the GA−HT complexes and the interaction of this amino acid with HT and, by inference, other LDH compounds. The most important points are the following. All the HT samples synthesized between pH 8.0 and 12.1 contain substantial amounts of GA, as demonstrated by compositional analysis, TGA−DTA, and ^{13}C NMR. XRD shows that the largest GA incorporation into the HT interlayers occurs at temperatures between 50 and 70 °C and at pH values near 10 and that a substantial amount of the HT structural charge is compensated by small, inorganic anions at all pH. At low pH, this anion is principally NO_3^-,

and at high pH, especially near 12, CO_3^{2-} and OH^- play important roles. ^{13}C NMR shows the presence of CO_3^{2-} in many samples, but the amounts cannot be determined quantitatively. The decrease in the $^1H-^{13}C$ CP-MAS signal intensity for GA at 100% RH suggests that much of the GA in all samples occurs on HT particle surfaces and that at high and low pH, most of it is on surfaces. The nearly total loss of signal for the pH 12.1 sample at 100% RH suggests that the GA on exterior surfaces of HT particles enters the surface fluid film that forms under these. This conclusion is consistent with the absence of XRD basal spacings for GA−HT under these conditions, especially at pH 8 and 12. The crystallinity of the HT samples is poor at pH 8 and 9 but improves at higher values, as shown by XRD.

The ^{13}C NMR chemical shifts of HT-associated glutamate are quite similar to those of glutamic acid in bulk aqueous solution, indicating that it does not cross-link (form covalent bonds with) the Mg and Al hydroxide layers under any conditions used here. The ^{13}C MAS and $^1H-^{13}C$ CP-MAS spectra resolve signals for both the β- and γ-CH_2 and COO^- sites of GA^{-1} and GA^{-2} anions associated with HT. However, the real GA^{-2}:GA^{-1} ratio has been determined only in single-pulse ^{13}C NMR experiments on a ^{13}C-enriched sample. It appears that this ratio is close to 1 for samples synthesized at pH about 10. At that pH, the GA^{-2}:GA^{-1} ratio in solution is expected to be greater than 1, probably indicating a preferential adsorption of GA^{-1}.

XRD basal spacings for GA−HT samples equilibrated at relative humidities from near 0% (over P_2O_5) to near 100% (over deionized water) suggest that at low water contents, interlayer glutamate lies with its long direction parallel to the hydroxide layers, whereas near normal room conditions and at 79% RH, increasing water contents allow glutamate to have its long axis at a high angle to these layers. At near 100% RH, low-angle XRD shows swelling to large spacings, suggesting that the GA molecules are not simultaneously in contact with the two metal hydroxide layers on the two sides of the interlayer gallery.

Acknowledgment. We thank Dr. A. G. Kalinichev, Dr. P. K. Babu, Dr. P. K. Padmanabhan, Dr. X. Hou, and Mr. Q. Li for many useful discussions concerning the structure of layered double hydroxide compounds. Dr. P. K. Babu is gratefully acknowledged for helping us record the ^{13}C-enriched sample NMR data on the 600 MHz spectrometer. We are thankful to four unknown reviewers who have greatly improved the quality of this paper with their comments and suggestions. This work was supported by Grant DEFG02-00ER15028 from the Geoscience Program of the U.S. Department of Energy Division of Basic Energy Sciences. Lower-angle XRD experiments were carried out at the Center for Microanalysis of Materials, University of Illinois, which is partially supported by the U.S. Department of Energy under Grant DEFG02-91-ER45439.

CM052107X